Cement & Concrete Composites 33 (2011) 778–787

Contents lists available at ScienceDirect

Cement & Concrete Composites

journal homepage: www.elsevier.com/locate/cemconcomp

Pore structure features of pervious concretes proportioned for desired porosities and their performance prediction

Milani S. Sumanasooriya [a], Narayanan Neithalath [b,*]

[a] Department of Civil and Environmental Engineering, Clarkson University, Potsdam, NY 13699, United States
[b] School of Sustainable Engineering and the Built Environment, Arizona State University, Tempe, AZ 85286, United States

ARTICLE INFO

Article history:
Received 22 February 2011
Received in revised form 31 May 2011
Accepted 2 June 2011
Available online 17 June 2011

Keywords:
Pervious concrete
Porosity
Granulometry
Pore size
Pore connectivity
Permeability
Katz–Thompson equation

ABSTRACT

The pore structure features such as the pore volume fractions, pore sizes, specific surface areas, and connectivity dictate the properties of any porous material. In this paper, an analysis of the pore structure features of pervious concretes designed for similar porosities using two different proportioning methods – one with higher paste contents and lower compactive efforts and another with lower paste contents and higher compactive efforts – is carried out. The porosities (both from volumetric and image analysis based methods) and characteristic pore sizes obtained from morphological functions are found to be statistically similar for the high-paste and low-paste content mixtures, while the low-paste content mixtures show a higher specific surface area of pores. The extracted pore structure features, when used in the Katz–Thompson equation for permeability prediction, result in over-estimation of permeability for specimens with larger pore sizes. A correction factor for the Katz–Thompson constant is found to be linearly related to the granulometry-based pore sizes.

1. Introduction

Pervious concrete, also known as no-fines concrete, or Enhanced Porosity Concrete (EPC) is well recognized as one of the key elements of low-impact sustainable development. The large, open pore structure (15–25% porosity, and pores of sizes ranging from 2 mm to 8 mm) of this material, resulting from the use of gap-graded coarse aggregates, low water-to-cementing materials ratio (w/c) and generally the absence of fine aggregates, allows transport of water through its structure, thereby helping reduce the adverse effects of storm-water runoff [1]. The tortuous interconnected pore network is also capable of reducing the tire-pavement interaction noise in concrete pavements [1–3], and the effect of urban heat islands [4]. While several studies have reported the results of mechanical and functional performance of pervious concretes, the material design has largely been based on trial-and-error or empirical procedures [1,3,5–8].

Material design of pervious concretes differs from that of conventional concretes in that a certain non-minimal porosity needs to be retained in the material structure for adequate performance levels. Since porosity is one of the prominent pore structure features of any porous material that is relatively easy to measure (especially in systems with large open porosity such as pervious concretes), it is beneficial to design pervious concrete mixtures for a desired porosity. Moreover, the relationship of porosity to the most important functional performance of the material, i.e., permeability, is well established [1,5,6,9,10]. Recently, particle-packing based material design methodologies have been developed to proportion laboratory pervious concretes for desired porosities [10,11]. Since the porosity of pervious concretes depends on the compaction effort applied, in addition to the solid material volume fractions, the recently developed proportioning procedure deals with two distinct types of pervious concretes: (i) mixtures, where a lower compactive effort is applied, i.e., the compaction level specified in ASTM C 1688 which is the standard for determination of voids content and unit weight of pervious concrete is used, thereby resulting in higher paste contents to achieve the desired porosities and (ii) mixtures, where a higher compactive effort than that prescribed in ASTM C 1688 is used, thus increasing the aggregate volume fraction in the mixture, resulting in reduced paste contents for the desired porosities. The pervious concrete mixtures resulting from these two distinct proportioning strategies are referred to as high-paste content mixtures and low-paste content mixtures, respectively in the remainder of this paper. It is expected that the differences in volume fractions of the components and the compaction effort would lead to differences in pore structure features between the high-paste and low-paste content pervious concrete mixtures. Since the pore structure features of such a random composite material significantly influences the mechanical [7,12] and transport [9,13–15] properties, it is desirable to carry

* Corresponding author. Tel.: +1 480 965 6023; fax: +1 480 965 0557.
E-mail address: Narayanan.Neithalath@asu.edu (N. Neithalath).

0958-9465/$ - see front matter © 2011 Elsevier Ltd. All rights reserved.
doi:10.1016/j.cemconcomp.2011.06.002

Nomenclature

v_{agg}	volume of coarse aggregates in a unit volume	R_b	bulk electrical resistance of the specimen
$v_{void\text{-}agg}$	volume of voids in a unit volume of compacted aggregates	σ_{eff}	effective electrical conductivity
$v_{paste\text{-}min}$	hypothetical minimum paste volume fraction	σ_0	electrical conductivity of the electrolyte
$(\Delta v)_{max}$	maximum additional paste volume fraction	β	pore connectivity factor
$(\Delta v)_{min}$	minimum additional paste volume fraction	d_{crit}	critical pore size determined using granulometric density function
ϕ_d	design porosity	$S_2(l)$	two-point correlation function
ϕ_{fresh}	fresh porosity determined based on ASTM C 1688	l	length of line segments used to obtain TPC function
ϕ_{hardened}	hardened state porosity	l_{TPC}	correlation length
ϕ_V	volumetric porosity	d_{TPC}	average pore diameter determined using TPC function
ϕ_A	area fraction of pores	s_p	specific surface area of the pores
f'_c	compressive strength	l_c	characteristic length scale of the porous medium
K	hydraulic conductivity	f	correction factor for the pore sizes used in K–T equation
k	intrinsic permeability		

out a detailed study on the important pore structure features of these concretes, and establish relationships with performance, which is the intention of this paper.

2. Mixture proportions and test methods

Type 1 ordinary Portland cement conforming to ASTM C 150 and crushed limestone aggregates were used to proportion the pervious concrete mixtures used in this study. The aggregate sizes used were: #8 (passing through 4.75 mm sieve, retained on 2.36 mm sieve), #4 (passing through 9.5 mm sieve, retained on 4.75 mm sieve), and 3/8″ (passing through 12.5 mm sieve, retained on 9.5 mm sieve).

2.1. Mixture proportioning methodologies for desired porosities

The foundations of the mixture proportioning approach for high-paste and low-paste content pervious concretes are summarized here. Assume that the coarse aggregates are compacted in accordance with the ASTM C 29 procedure (for the determination of bulk density and voids in aggregates) to provide a volume fraction of v_{agg} in a unit volume as shown in Fig. 1a. The void volume fraction can then be given as: $v_{void\text{-}agg} = 1 - v_{agg}$. If the compaction method corresponding to ASTM C 29 is employed in the proportioning of pervious concrete mixtures, then the volume fraction of paste required to maintain a desired porosity of ϕ_d ($\phi_d < v_{void\text{-}agg}$) can be expressed as: $v_{paste-\min} = v_{void-agg} - \phi_d$. Understandably, this is the hypothetical minimum paste volume fraction because the aggregates are compacted to (almost) their maximum packing densities [10]. This is shown in Fig. 1b. However, the standard methodology for the determination of fresh porosity of pervious concrete, ASTM C 1688, recommends a compactive effort (two layers in a 0.007 m^3 container, 20 drops of proctor hammer per layer) which is much lower as compared to the ASTM C 29 procedure of compacting aggregates. This results in a lower aggregate volume per unit volume of the pervious concrete mixture, and consequently increased porosities than the desired values. If the compaction effort has to remain the same as that suggested in ASTM C 1688, additional paste volume fraction would be required to achieve the desired porosities (assuming the paste to be relatively incompressible) as shown in Fig. 1c. The mixtures thus proportioned, using an additional paste volume fraction of $(\Delta v)_{max}$ are termed as high-paste content mixtures. The value of $(\Delta v)_{max}$ was found to be about 0.09 irrespective of the aggregate sizes and desired porosities [10,11]. The average compaction energy provided for these mixtures was calculated to be 42.6 kN m/m^3.

In an attempt to ensure reduced cement consumption in pervious concretes, another proportioning method was adopted, wherein the compaction effort was increased along with a reduction in the paste content to achieve the desired porosities. The compaction effort was increased from the ASTM C 1688 level of two layers in a 0.0.007 ft^3 container and 20 drops of proctor hammer per layer to 3 layers and 30 drops of proctor hammer per layer, providing an average compaction energy of 95.8 kN m/m^3, i.e., double the energy provided for the high-paste content mixtures. It was also

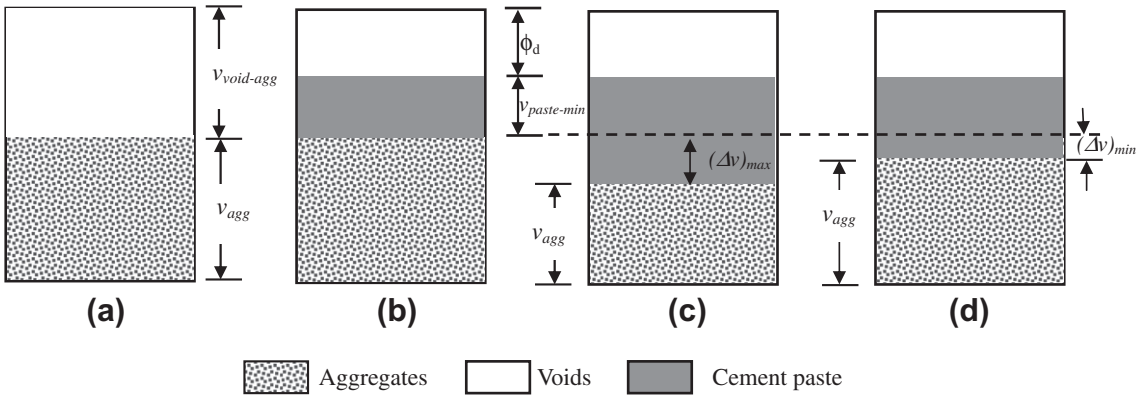

Fig. 1. Illustration of the differences in aggregate, cement paste, and void volume fractions when compacted according to: (a) ASTM C 29 procedure (aggregate only), (b) ASTM C 29 procedure (with the hypothetical minimum paste volume), (c) ASTM C 1688 compaction procedure (high-paste content mixtures), and (d) modified compaction procedure (low-paste content mixtures).

found that desired porosities cannot be achieved using a paste volume fraction of $v_{paste\text{-}min}$, and hence it was augmented by $(\Delta v)_{min}$ as shown in Fig. 1d. The value of $(\Delta v)_{min}$ typically ranged between 0.02 and 0.04 depending on the aggregate sizes. The mixtures thus proportioned are termed as low-paste content mixtures.

Following the above mentioned proportioning procedures, several trial mixtures were prepared to ascertain if the fresh porosities, ϕ_{fresh} (determined based on ASTM C 1688) matched the design porosities (ϕ_d). The final proportions for both the high-paste and low-paste content pervious concrete mixtures are shown in Table 1. Both the mixture proportioning methods explained here were capable of achieving porosities close to the design porosities (between 19% and 27%) as shown in this table.

To prepare the specimens in cylinders for strength determination, the compactive effort was adjusted so that the fresh porosity (in 0.007 m^3 containers as per ASTM C 1688) and the hardened porosity (measured using the volumetric method in 100 mm diameter × 200 mm long cylinders) would be comparable. It was found that for the high paste content mixtures, a compactive effort of five drops of Proctor hammer per layer for two layers in the cylindrical molds was sufficient to bring the hardened state porosities close to the design porosity (and the fresh porosity), whereas for the low paste content mixtures, the compactive effort required to achieve the same was eight blows per layer for three layers. The mixtures were filled in 100 mm diameter × 200 mm long cylindrical molds for compressive strength determination and image analysis procedures. For the specimens to be used for porosity, permeability, and pore connectivity determination, an inner sleeve was placed inside the molds to reduce the specimen diameter to 95 mm. The specimens were removed from the molds after 24 h and allowed to cure in a moist chamber at a RH > 98% until the age of testing. The compressive strengths of the hardened specimens were determined at an age of 28 days using a 490 kN closed-loop universal testing machine operating in displacement controlled mode, at a strain rate of 100 με/s. The compressive strengths of the high-paste and low-paste content pervious concrete mixtures are also shown in Table 1.

2.2. Determination of volumetric porosity, permeability, and effective electrical conductivity

The effective volumetric porosities (ϕ_V) of the pervious concrete specimens were determined using a well-reported procedure, where the mass of water required to fill the pores in a pervious concrete specimen enclosed in a latex sleeve is measured [1,16]. For a particular pervious concrete mixture, three specimens were used for porosity determination and the average value is reported. The hydraulic conductivities (K, in m/s) of pervious concrete mixtures were determined using a falling head permeameter, the details of which have been extensively published [1,9,16,17]. The hydraulic conductivity (K) was converted into intrinsic permeability (k in mm^2) using the density and viscosity of water along with the acceleration due to gravity.

Alternating current (AC) electrical impedance spectroscopy measurements (using a Solartron™ frequency response analyzer) were carried out on pervious concrete mixtures to obtain the effective electrical conductivity (σ_{eff}) so as to facilitate the determination of the connectivity of the pore system. The measurements were carried out on 95 mm diameter × 150 mm long specimens by filling the pores with an electrolyte (NaCl) of known conductivity (3% NaCl, with a σ_0 of 4.4 S/m was used in this study). The experimental details can be found elsewhere [9,16,18]. The bulk resistance of the specimen (R_b) is obtained from the meeting of the bulk and electrode arcs in a Nyquist plot (which plots the real vs. imaginary impedance for a range of frequencies). The effective electrical conductivity (σ_{eff}) is then obtained using the values of the measured bulk resistance and the specimen geometry. The measured porosity (ϕ_V), and the conductivity of the electrolyte (σ_0) were used along with σ_{eff} to determine the pore connectivity factor (β) as:

$$\beta = \frac{\sigma_{eff}}{\sigma_0 \phi_V}. \quad (1)$$

2.3. Image processing and analysis to extract the pore structure features

Image analysis has been widely used in the pore structure characterization of pervious concretes [9,13,19,20]. For image analysis, 100 mm diameter × 150 mm long specimens were sectioned into 50 mm thick slices. For a particular pervious concrete mixture, two to three cylinders were used, and thus 6–18 surfaces were obtained. The surfaces were ground to obtain a smooth surface, and the solid phase was painted in white. These surfaces were scanned over a clear plastic film in gray scale mode using a flat bed scanner

Table 1
Mixture Proportions for 1 m^3 of pervious concrete, the fresh and hardened porosities, and the compressive strengths for the high-paste content and low-paste content mixtures.

Aggregate composition	Design porosity (ϕ_d)	Cement (kg/m^3)	Water (kg/m^3)	Aggregates (kg/m^3)	Fresh porosity (ϕ_{fresh})*	Volumetric porosity (ϕ_V)#	28-day Compressive strength (f'_c) (MPa)
High-paste content mixtures							
100% #8	0.19	554	180	1263	0.192	0.183 (0.002)	19.89 (1.50)
	0.22	496	163	1279	0.202	0.211 (0.008)	14.65 (1.48)
	0.27	411	137	1286	0.265	0.255 (0.007)	9.66 (0.25)
100% #4	0.19	560	181	1253	0.196	0.169 (0.010)	20.60 (1.86)
	0.22	492	161	1285	0.219	0.223 (0.012)	15.89 (0.44)
	0.27	414	138	1281	0.261	0.256 (0.006)	9.30 (0.59)
100% 3/8″	0.19	539	175	1289	0.197	0.195 (0.003)	19.13 (0.41)
	0.22	485	160	1297	0.214	0.238 (0.004)	15.66 (1.87)
	0.27	398	133	1307	0.268	0.246 (0.003)	7.55 (2.06)
Low-paste content mixtures							
100% #8	0.22	317	101	1579	0.235	0.202 (0.013)	12.51 (1.20)
100% #4	0.19	345	109	1612	0.196	0.195 (0.004)	17.61 (2.05)
	0.22	297	95	1634	0.233	0.242 (0.016)	13.20 (0.85)
	0.27	216	71	1652	0.272	0.289 (0.013)	7.70 (0.45)
100% 3/8"	0.19	336	107	1628	0.195	0.178 (0.023)	17.01 (0.31)
	0.22	287	92	1647	0.211	0.242 (0.016)	12.24 (0.62)
	0.27	206	68	1683	0.271	0.264 (0.004)	6.90 (0.76)

The figures in the parenthesis represent one standard deviation for ϕ_V or f'_c values corresponding to two or three specimens from a certain mixture.
* Determined using ASTM C 1688 procedure.
# Determined in the hardened state.

at a resolution of 300 dpi. The images without any edge effects were further processed using an image processing and analysis software (ImageJ™) [21]. The gray scale images were cropped into circular images of 570 pixels (95 mm) diameter, and thresholded to obtain binary images (showing the pore and solid phases) by analyzing the gray level histogram. The binary images were further cleaned to remove the noise. From these processed circular images, 400 pixel × 400 pixel square images were extracted and used to obtain the pore structure features. Adequacy of this image processing procedure in providing representative images corresponding to different pervious concrete mixtures for feature analysis has been quantified in [13,19].

2.3.1. Area fraction of pores, pore sizes, and specific surface area

For two-dimensional images, the image analysis software measures the area of each individual pore, sums them up, and divides it by the total area of the image, to provide the pore area fraction (ϕ_A). For a particular pervious concrete mixture, ϕ_A values for all the two-dimensional images were obtained and the average value is reported.

The characteristic pore sizes for pervious concrete mixtures were extracted using granulometric density and two-point correlation (TPC) functions [9,19]. The granulometric density function is a well known morphological method that can be used to characterize the feature size distribution in two-dimensional images [22,23]. The use of opening granulometric density functions for obtaining the characteristic pore size of pervious concretes has been discussed in previous studies [9,19]. The method involves the use of structuring elements (SE) (circular SEs are used in this study) of increasing sizes to "open" the image, i.e., when the image is opened using a SE of diameter "x" mm, all pores less than "x" mm are removed from the image. The result is a plot of the area fraction of pores remaining as a function of the size of SE. The size of the SE corresponding to the local maximum in the discrete 1st derivative of this relationship is the critical size of the opening (d_{crit}) that corresponds to the smallest pore that completes the first connected pathway in the material. In other words, d_{crit} is related to the percolation threshold of porosity in the material [24].

TPC function is another morphological means of feature estimation and it contains information about area fraction of pores, characteristic pore sizes, and the specific surface area of the pores. The use of TPC functions in image analysis-based performance prediction of porous materials can be found in [25–27]. The TPC function for a two-phase material can be obtained by randomly throwing line segments of length "l" with a specific orientation into the structure and counting the fraction of times the end points of the line lie in the phase of interest [28]. Fig. 2 shows a typical TPC function [$S_2(l)$] for a pervious concrete mixture. The area fraction of the image (ϕ_A) is given by the value at $l = 0$ [$S_2(l = 0)$]. The correlation length (l_{TPC}) is defined as the abscissa of the intersection point of the slope of TPC function at $l = 0$ and the horizontal asymptote at which $l \to \infty$ (Fig. 2). l_{TPC} can be related to the average pore diameter (d_{TPC}) as:

$$d_{TPC} = l_{TPC}/(1 - \phi_A) \tag{2}$$

The specific surface area of the pores (s_p), defined as the total pore surface area for a unit volume of the material, can also be extracted from the TPC function. The slope of $S_2(l)$ at $l = 0$ is related to s_p as [28,29]:

$$\lim_{l \to 0} \frac{\partial S_2(l)}{\partial l} = -\frac{s_p}{4} \tag{3}$$

3. Results, analysis and discussions

3.1. Analysis of pore structure features of high-paste and low-paste content pervious concrete mixtures

A comparison of the pore structure features such as the volume and area fractions, characteristic pore sizes, and specific surface area of high-paste and low-paste content pervious concrete mixtures are provided in this section.

3.1.1. Volumetric porosity (ϕ_V) and area fraction of pores (ϕ_A)

Porosity is one of the most important pore structure parameters of porous materials, as it can be directly related to the material performance. The volumetric porosities (ϕ_V) and area fraction of pores (ϕ_A) were obtained for all the high-paste and low-paste content mixtures using the procedures explained in Section 2. Fig. 3 shows a comparison of the volumetric porosities (ϕ_V) and area fraction of pores (ϕ_A) for the high-paste and low-paste content pervious concrete mixtures. It can be seen from this figure that ϕ_A values of high-paste and low-paste content pervious concrete mixtures are in a reasonable agreement with the corresponding volumetric porosities (ϕ_V). This is in conformance with the stereological theory

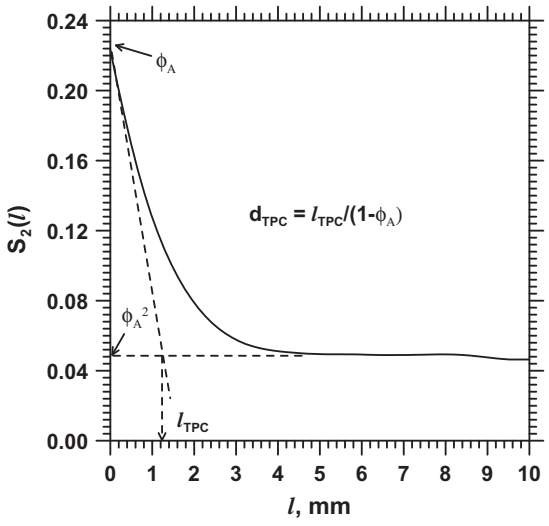

Fig. 2. Two-point correlation function of a typical two-dimensional image of a pervious concrete mixture (100% #8, ϕ_V = 21.9%, ϕ_A = 22.0%).

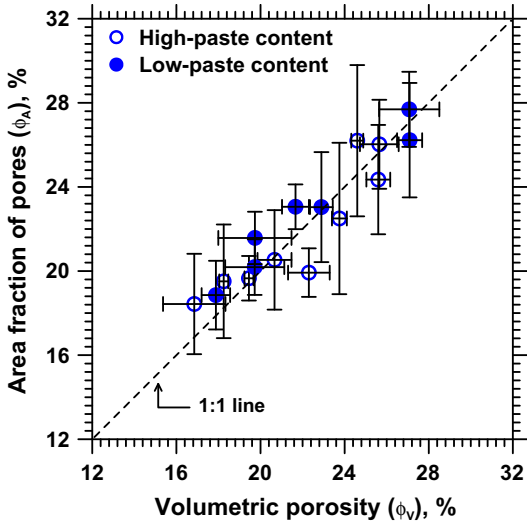

Fig. 3. Relationship between the pore volume and area fractions for the pervious concrete mixtures proportioned using both the methods.

which states that, if a statistically significant number of random samples are used, the area fraction of pores should be similar to the volumetric porosities [30]. The horizontal error bars in Fig. 3 indicate one standard deviation for ϕ_V values corresponding to three specimens corresponding to the same mixture, and the vertical error bars indicate one standard deviation for ϕ_A values of three to seventeen images corresponding to a certain mixture.

3.1.2. Characteristic pore sizes and pore specific surface area

As mentioned in an earlier section, TPC and granulometric density functions were used to extract the characteristic pore sizes from two-dimensional images of pervious concrete cross sections. Fig. 4a and b show the characteristic pore sizes determined using TPC functions (d_{TPC}) and granulometric density functions (d_{crit}), respectively for the high-paste and low-paste content pervious concrete mixtures. A general trend of increasing pore sizes (both d_{TPC} and d_{crit}) with increasing aggregate sizes can be easily noticed. For a certain aggregate size, increase in porosity is generally not found to result in a considerable increase in the pore sizes, for a given proportioning method. This could be attributed to the fact that the compaction method is the same for a given proportioning method. It can also be noticed from Fig. 4a and b that the pore sizes (both d_{TPC} and d_{crit}) are slightly lower for the low-paste content mixtures, because of the increased consolidation effort (see Section 2.1) provided to these mixtures. The statistical similarity of the pore sizes obtained for the mixtures proportioned differently will be discussed in a later section. Based on Fig. 4a and b, it can be stated that d_{TPC} and d_{crit} values are reasonably close to each other, facilitating the use of either of these parameters as a representation of pore size in pervious concrete mixtures. Similar results are reported in [9,19].

Fig. 5 shows pore specific surface areas (s_p) of the pervious concrete mixtures proportioned using the two different proportioning methods. As can be seen from Fig. 5, s_p is found be higher for the mixtures designed for larger porosities using a certain aggregate size. Since there is no significant difference between the pore sizes of pervious concretes made using a certain aggregate size irrespective of the porosities (for both high-paste and low-paste content mixtures, see Fig. 4), the number of pores in a unit volume of pervious concrete should be higher for the mixtures designed for larger porosities, in order to account for the increase in porosity. Thus, the total pore surface area in a unit volume of concrete in such mixtures is higher, which results in a higher s_p. Also, the s_p values are found to be relatively higher for the low-paste content mixtures as compared to the high-paste content mixtures, for the following reason. If pervious concrete mixtures are proportioned for a desired porosity, the number of pores in a unit volume of the low-paste content mixture should be higher as compared to that in the high-paste content mixture, in order to preserve the desired porosity, as the characteristic pore sizes are slightly lower (even though

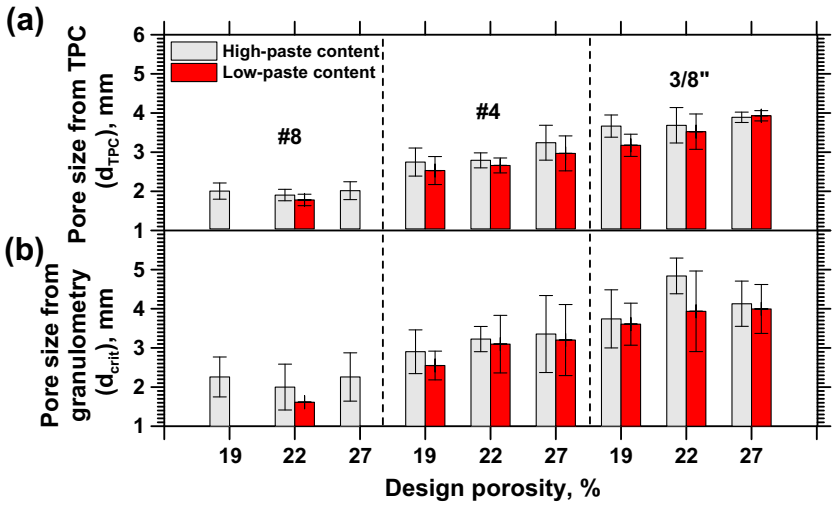

Fig. 4. Pore sizes determined using: (a) two-point correlation function and (b) opening granulometry, for high-paste and low-paste content mixtures of different design porosities.

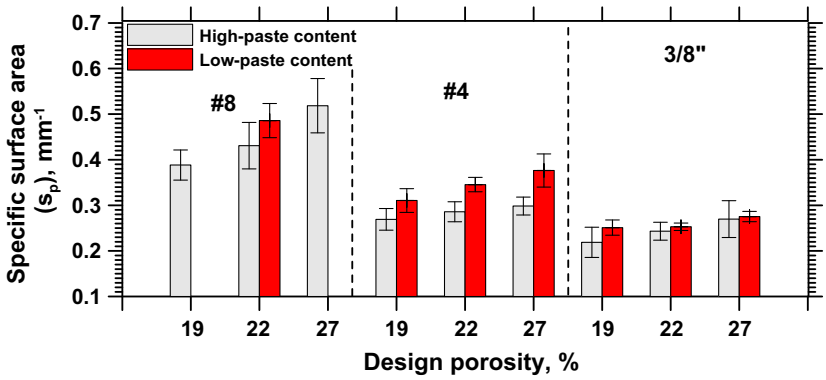

Fig. 5. Specific surface areas of the high-paste and low-paste content mixtures of different design porosities.

there is not a large difference) for the low-paste content mixtures. Lower pore sizes, and a greater number of pores contribute to an increase in the total pore surface area per unit volume.

3.1.3. Statistical analysis of the similarity in pore structure features between high-paste and low-paste content mixtures

In order to determine the statistical similarity between the pore structure features of high-paste and low-paste content mixtures, a detailed statistical analysis was carried out using the two-sample t-test. This test can be used determine whether the pore structure features corresponding to two methods are likely to have come from distributions with equal population means. The null hypothesis in a two-sample t-test is that the two data sets come from distributions with equal population means [31]. The test results in a *p*-value, which is defined as the smallest level of significance that would lead to a rejection of the null hypothesis. A *p*-value greater than 0.05 indicates that the null hypothesis can be accepted at a level of significance of 0.05 (i.e., at a 95% confidence level). The summary of the observed *p*-values for the different pore structure features are given in Table 2. The *p*-values that are lower than 0.05 are shown in bold in this table. It is observed that the porosities (ϕ_V and ϕ_A) and characteristic pore sizes (d_{crit} and d_{TPC}) of high-paste and low-paste content mixtures are statistically similar. The fact that there is no statistical difference between the measured porosities of specimens proportioned using both the proportioning approaches confirms the adequacy of these proportioning methods. Though Fig. 4a and b have shown that the low-paste content mixtures have slightly smaller pore sizes, the t-test shows that the means are not statistically different between the high-paste and low-paste content mixtures. However, for specific surface area, the t-test shows that the means of the high-paste and low-paste content mixtures are generally different. Even though there is only a marginal difference in the pore sizes, they contribute to appreciable changes in the surface area of the pores. For mixtures made using larger aggregates (i.e., having larger pore sizes), no statistical difference in specific surface areas is noticed. This is because, when the pore size is large, the number of pores for a given porosity are lower, which correspondingly results in smaller changes in the specific surface area.

3.2. Connectedness of the pore structure

The connectedness of the pore structure in porous materials can be expressed using an experimentally determined pore connectivity factor (β). β plays an important role in determining the transport properties of porous materials such as pervious concretes [9,16]. Higher β has been shown to essentially result in higher permeability, even though the permeability is dependent on several other pore structure features. The pore connectivity factors of the pervious concrete specimens used in this study were determined using Eq. (1). Fig. 6 depicts the variation in β for the high-paste and low-paste content pervious concrete mixtures proportioned using different aggregate sizes and designed for different porosities. For the same aggregate size (or the same pore size), increase in the porosity increases the effective electrical conductivity [32] and thus the pore connectivity factor. For the same porosity, an increase in aggregate size (or pore size) is also found to increase the pore connectivity factor. Increasing pore sizes at the same porosity translates into a fewer number of larger pores. The measured effective conductivities of larger pore size systems are observed to be higher than those of systems with smaller pore size at similar porosities, thereby resulting in higher connectivities as per Eq. (1). For the smaller pore size system (or, larger number of pores at the same porosity), the measured conductivity is lower because of the presence of the larger number of throats connecting the pores [33], consequently lowering the pore connectivity factor.

Table 2
Summary of the *p*-values obtained from a two-sample t-test for the high-paste and low-paste content pervious concrete mixtures.

Aggregate Composition	Design porosity (%)	Resultant *p*-values from t-test for different pore structure features				
		Volumetric porosity (ϕ_V) (2–3 specimens)	Area fraction of porosity (ϕ_A) (3–17 images)	Critical pore size (d_{crit}) (3–17 images)	Pore size from TPC (d_{TPC}) (3–17 images)	Specific surface area (s_p) (3–17 images)
100% – #8	22	0.461	0.249	0.066	0.053	**0.018**
100% – #4	19	0.536	0.794	0.411	0.396	**0.037**
	22	0.506	0.090	0.607	0.267	**0.007**
	27	0.207	0.284	0.770	0.323	**0.001**
100% – 3/8″	19	0.382	0.637	0.727	**0.003**	**0.047**
	22	0.122	0.719	0.081	0.663	0.362
	27	0.351	0.988	0.678	0.756	0.734

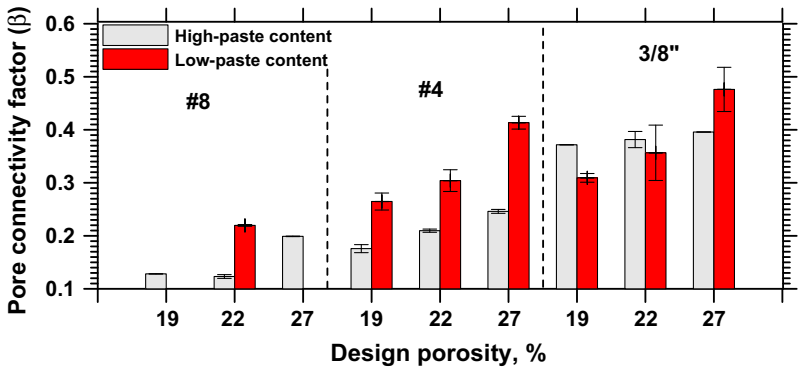

Fig. 6. Pore connectivity factors of the high-paste and low-paste content mixtures of different design porosities.

The observations of Fig. 6 show that pore connectivity factor can be used a convenient experimental measure to quantify the connectedness of the pervious concrete pore structure.

In general, Fig. 6 shows that the high-paste content mixtures have a lower pore connectivity factor which can be attributed to paste clogging. The permeability measurements, shown later in this paper also supports this observation. Higher amounts of paste can be expected to drain through the pore structure, resulting in a paste-rich lower layer in pervious concrete specimens, which was visually observed for the high-paste content mixtures. A quantification of paste draining is presented here using the variation of pore and paste area fractions along the depth of high-paste content pervious concrete mixtures. Image analysis was performed on vertical slices from 150 mm long cylindrical specimens. The 150 mm long × 95 mm wide rectangular sections were thresholded to separate the pore and solid phases as shown in Fig. 7a. These images were divided into 25 mm deep × 95 mm wide strips, and the pore area fractions in each of the strips were determined. To determine the paste volume fractions, the cut sections were sprayed with phenolphthalein to distinguish between the cement paste and aggregates. These sections were then subjected to image analysis using a color thresholding procedure. The color thresholded image, where the paste area was separated from the remaining features was then converted to a binary image as shown in Fig. 7b. The paste area fractions were also determined for every 25 mm deep × 95 mm wide strips along the depth. The variation of pore and paste area fractions along the depth for high-paste content mixtures using all three aggregate sizes, designed for 19% porosity are shown in the plots in Fig. 7a and b, respectively. The plotted values correspond to the average of pore area or paste area fraction measurements on six different vertical sections obtained from hardened specimens corresponding to each mixture. It can be noticed that the pore area fraction decreases and paste area fraction increases along the depth of the specimens for all the high-paste content mixtures. A minimum porosity, and correspondingly a maximum paste area fraction, is observed at the bottom of the specimen, confirming that paste clogging occurs near the bottom of the specimens. Similar trends were observed for the mixtures proportioned for 27% porosity also; however, the variation in the pore and paste area fractions with depth were lower for such mixtures since the amount of paste used was lower compared to the mixtures proportioned for 19% porosity. Paste clogging was not observed either visually or through image analysis on a few vertical slices for the low paste content mixtures.

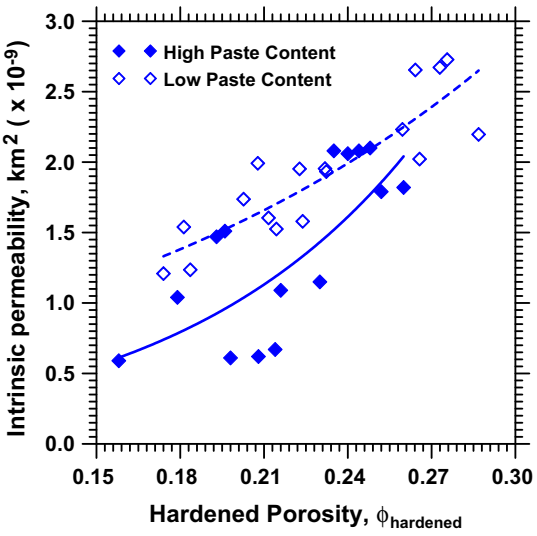

Fig. 8. Intrinsic permeability as a function of the porosity for the high-paste and low-paste content pervious concrete mixtures.

3.3. Permeability predictions based on pore structure features

Fig. 8 shows the relationship between intrinsic permeability (k) and volumetric porosity (ϕ_V) for all the pervious concrete mixtures used in this study. Permeability increases with an increase in porosity, as expected. It can be observed from Fig. 8 that the intrinsic permeabilities are lower for the mixtures made with high-paste contents as compared to those made with low-paste contents. This could be attributed to the localized paste clogging in high-paste content mixtures that result in lower pore connectivity, which has been shown in the earlier section.

The Katz–Thompson (K–T) equation is commonly used to predict the permeability of porous materials [34]. For a porous medium with a characteristic length scale l_c, intrinsic permeability (k) can be expressed as:

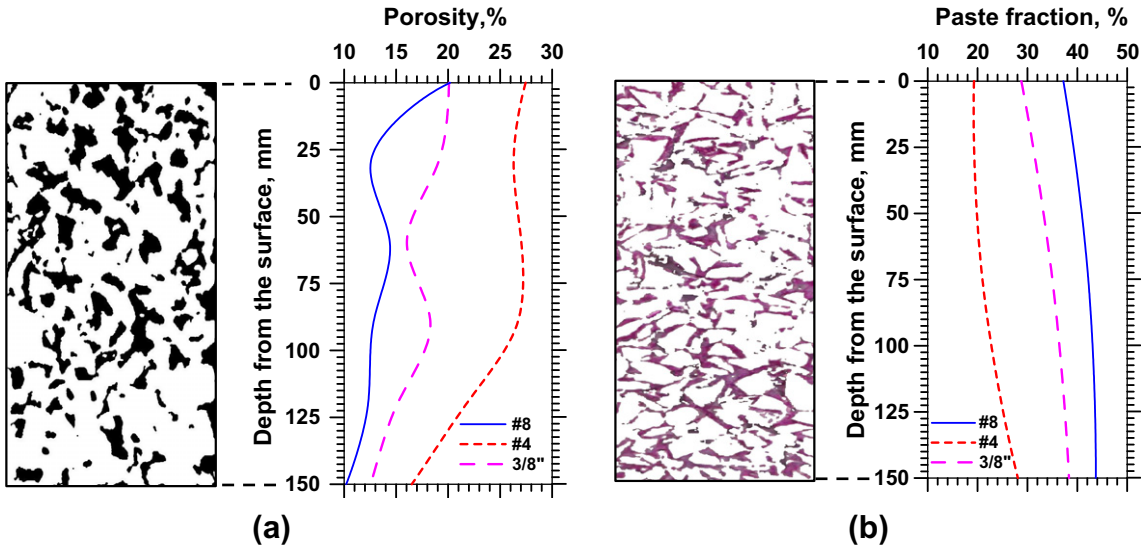

Fig. 7. Variation of: (a) pore area fraction and (b) paste area fraction with depth in a 19% porosity high-paste content pervious concrete mixture to confirm paste clogging. The pores are represented by the dark areas in the thresholded image in (a) and the paste is represented by the dark areas in the thresholded image in (b).

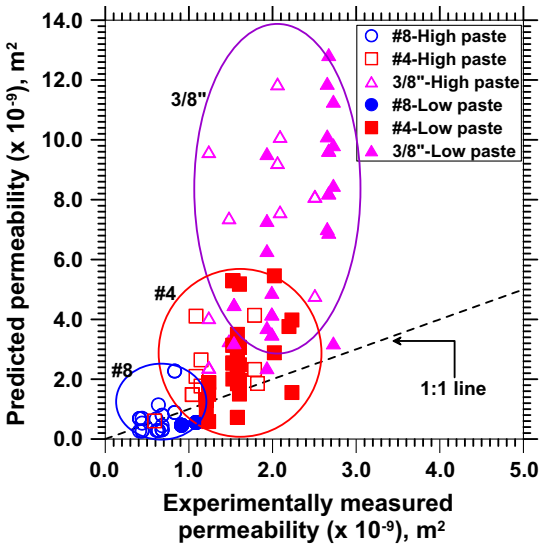

Fig. 9. A comparison of the experimentally determined permeabilities and those predicted by the standard Katz–Thompson (K–T) equation for high-paste and low-paste content pervious concrete mixtures. Notice the wider scatter for specimens made using larger sized aggregates,

$$k = \left(\frac{1}{226}\right)\frac{\sigma_{eff}}{\sigma_0} l_c^2 = \left(\frac{1}{226}\right)(\phi\beta)\cdot l_c^2 \quad (4)$$

$(\frac{1}{226})$ is a constant developed by Katz and Thompson for rock specimens based on a number of assumptions including the cylindrical nature of the pore geometry and an equivalence of local rock conductivity to the conductivity of the pore solution [34]. The other terms of this equation have been defined elsewhere in this paper. While the critical path analysis of transport in porous media [35], which is the precursor to the Katz–Thompson equation, assumed similar conduction pathways for electrical and fluid flow in the porous media, the K–T equation considers different electrical and hydraulic flow paths. The characteristic length scale, l_c, can be considered to be related to the percolating pore size in porous materials. Since the granulometric density function based pore size (d_{crit}) is a percolation related parameter, l_c is approximated using d_{crit} in this paper.

When the predicted permeabilities using σ_{eff}/σ_0 (or $\phi\beta$) obtained from electrical conductivity results and d_{crit} in Eq. (4) are plotted against the experimental permeabilities, a wide scatter is observed as shown in Fig. 9. A closer observation of this figure reveals some trends: (i) for the specimens made using #8 aggregates (i.e., having smaller pore sizes), the K–T equation as given in Eq. (4) predicts the permeabilities fairly adequately and (ii) the scatter is more for specimens made using larger aggregate sizes (i.e., larger pore sizes), and it decreases with a reduction in aggregate size. Explanations for this behavior are provided below.

In the development of the original K–T equation, it was considered that the conduction through pores of size less than l_c can be ignored [34]. When the pores are smaller and regular as is the case with specimens made using #8 aggregates ($d_{crit} \approx 2.0$ mm), for a certain porosity, there is quite a uniform distribution of pores [9,13,19]. The mean free spacing between the pores [9,19], which is a dispersion related parameter, is smaller when the pore sizes are smaller, as shown in Fig. 10a, also indicating better pore phase dispersion, as compared to the specimens with larger pore sizes (and aggregate sizes). Conduction is then dominated by the pores that are of the critical size and larger because of the low proportion of pores smaller than this size. See Fig. 10b which shows the pore size histograms for representative pervious concretes of 22% porosity made with all the three aggregate sizes. The distribution of pore sizes is narrower for the specimens made using smaller aggregate sizes and broader for the specimens made using larger aggregate sizes. This figure shows that 70% of the pores in the specimen made with #8 aggregates lie in the 1 mm–3 mm diameter range, i.e., the size distribution is relatively narrow. Since the pores are already smaller, the conductance through pores smaller than the critical size will be relatively lower, and can be neglected. This has also been verified in two-dimensional pore networks with narrow pore size distributions [35]. In this case, the system is closer to the idealized one assumed in the development of the K–T equation. Thus there is no need to change the constant (1/226) in Eq. (4). This is evident from the K–T predicted permeabilities of specimens with smaller aggregate sizes (or pore sizes) being comparable to the experimental values as shown in Fig. 9.

However, for the same porosity, if the critical pore size is larger as is the case with mixtures made using 3/8″ aggregate sizes ($d_{crit} \approx 4.0$ mm), the pores smaller than this size also might

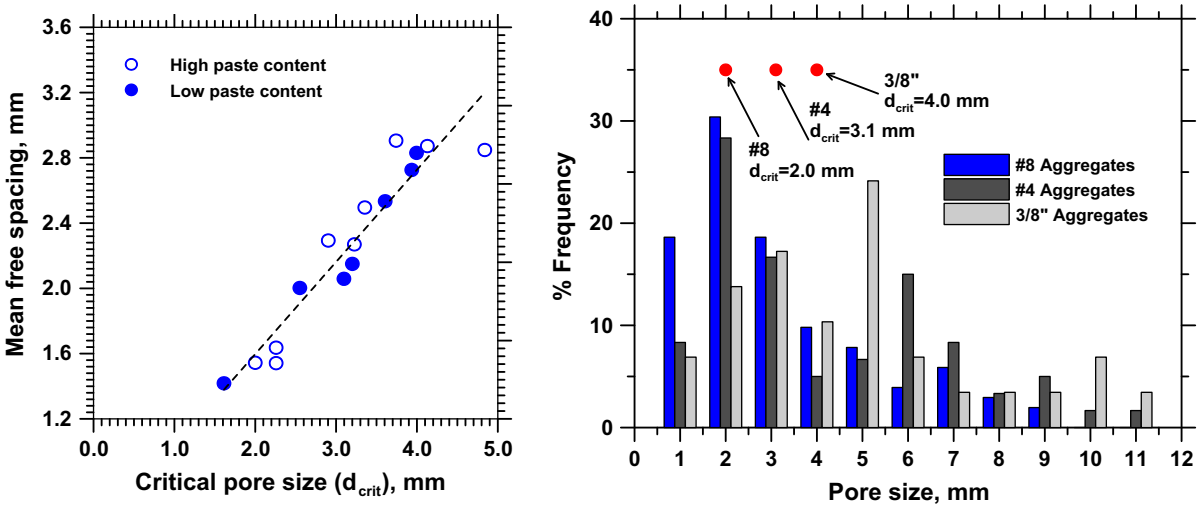

Fig. 10. (a) Mean free spacing of pores (a pore space dispersion parameter) as a function of the critical pore size and (b) histograms of pore size for specimens of 22% porosity, made using three different aggregate sizes. The symbols correspond to the critical pore sizes of each of the three different mixtures.

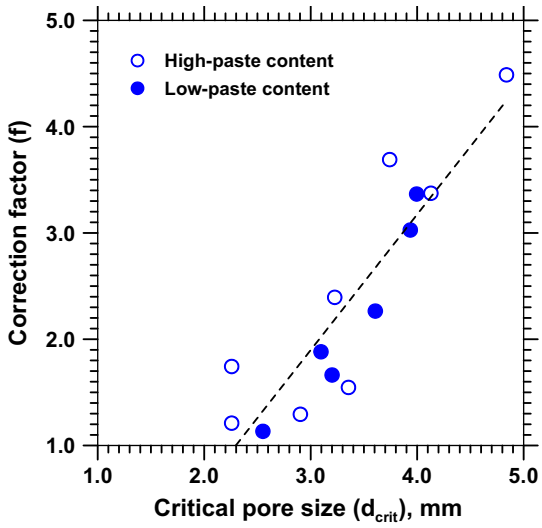

Fig. 11. Relationship between the percolation related pore size and a correction factor (ratio of the permeability predicted using Eq. (4) to that of the experimental permeability) that can be used in the denominator of the K–T equation.

facilitate a fair amount of conduction. From Fig. 10b, it can be seen that the size range that incorporates 70% of the pores is 1 mm–6 mm, and about 40% of the pores are smaller than d_{crit}. Here, the estimated d_{crit} using the granulometric density function could in fact be higher than the actual smallest percolating pore size, thus influencing the permeability predictions. Granulometry provides only a 2-D pore size distribution and provides little information on the apertures that connect the pores [36]. The above inference is also in agreement with [37], where the characteristic length scale l_c is reported to be much smaller than the percolation related diameter when there is a disorder in the diameter of pores, which is dominated by the disorder in the aspect ratio of pores. It was shown in previous studies [9,13] that the disorder in the aspect ratio of pores is more for specimens made using larger aggregate sizes, i.e., the pores tend to be more irregular with increasing sizes. This results in an over-estimation of permeabilities for specimens with larger pore sizes when the K–T equation is used. Since the square of the pore sizes (d_{crit}) is used in the K–T equation, it is not surprising that the scatter increases with the pore size. When a correction factor to be used along with the denominator in the K–T constant, expressed as the ratio of the permeability predicted using Eq. (4) to the experimental permeability, is determined, it shows a very good relationship with the critical pore sizes. This is shown in Fig. 11. While not a universal relationship, this facilitates an understanding of the limits under which the K–T equation can be adopted for permeability prediction of pervious concretes. It is anticipated that similar pore size – correction factor relationships could be extracted for random porous media so as to facilitate permeability prediction using a modified Katz–Thompson equation.

4. Conclusions

A detailed evaluation of the pore structure features that dictate the performance of pervious concretes proportioned for desired porosities using two different methods have been provided in this paper. The adequacy of these proportioning methods was ascertained through the similarities in design and actual porosities as well as the similarities in porosities between the mixtures proportioned differently. The salient conclusions are listed below:

(i). The two porosity determination methods – volumetric and image analysis-based, and the two different morphological means of pore size determination – opening granulometry and two-point correlation function resulted in statistically similar values for both the high-paste and low-paste content pervious concrete mixtures. Pore sizes were found to be influenced only by the aggregate size and not by the porosity. In general, there was a statistically significant difference in the specific surface area of pores between the high-paste and low-paste content pervious concrete mixtures, attributable to the magnified effect of the small differences in pore sizes (though the differences in pore sizes were statistically insignificant) between these mixtures when areas are determined.

(ii). The pore connectivity factor (β) determined from electrical measurements increased with increasing porosity and pore sizes for both the high-paste and low-paste content mixtures. The high-paste content mixtures had lower β values because of paste clogging, which was confirmed through image analysis on vertical cross-sections. Smaller aggregate sizes (and thus pore sizes) at a given porosity resulted in reduced connectivities because of the presence of a larger number of apertures or throats in such specimens, which contribute to reduced conductivity.

(iii). The high-paste content mixtures showed lower permeabilities because of the effect of paste-clogging that reduces the pore connectivity factor, thus providing two distinct porosity–permeability relationships for the high-paste and low-paste content mixtures, respectively. Application of the well-known Katz–Thompson (K–T) equation using the ratio of effective electrical conductivity to the electrolyte conductivity ($\sigma_{eff}/\sigma_0 = \phi\beta$) and the percolation related pore size from granulometry (d_{crit}) as the inputs along with the K–T constant of 1/226 resulted in over-estimation of intrinsic permeabilities, especially for the mixtures with larger aggregate (and pore) sizes. The possible over-estimation of the critical pore sizes in specimens made using larger aggregates, which leads to non-negligible conduction through pores smaller than the critical size was attributed to this observation. The correction factor required for the K–T constant was found to scale linearly with the critical pore size.

Acknowledgements

The authors sincerely acknowledge the support from National Science Foundation (NSF) for the conduct of this study through a CAREER award (CMMI 1129369) to the second author. Numerous discussions with Dale Bentz of the National Institute of Standards and Technology (NIST) are also acknowledged. The contents of this paper reflect the views of the authors who are responsible for the facts and accuracy of the data presented herein, and do not necessarily reflect the views and policies of the supporting agencies, nor do the contents constitute a standard, specification, or a regulation.

References

[1] ACI 522R, Report on pervious concrete (ACI 522R – 10). American Concrete Institute; 2010.
[2] Neithalath N, Marolf A, Weiss J, Olek J. Modeling the influence of pore structure on the acoustic absorption of enhanced porosity concrete. J Adv Concr Technol 2005;3(1):29–40.
[3] Marolf A, Neithalath N, Sell E, Wegner K, Weiss J, Olek J. Influence of aggregate size and gradation on acoustic absorption of enhanced porosity concrete. ACI Mater J 2004;101(1):82–91.
[4] Reducing urban heat islands: compendium of strategies – cool pavements; <http://www.epa.gov/heatisland/resources/pdf/CoolPavesCompendium.pdf> (accessed 26.05.11).

[5] Meininger RC. No-Fines pervious concrete for paving. Concr Int 1988;10(8):20–7.
[6] Yang J, Jiang G. Experimental study on properties of pervious concrete pavement materials. Cem Concr Compos 2003;33:381–6.
[7] Deo O, Neithalath N. Compressive behavior of pervious concretes and a quantification of the influence of random pore structure features. Mater Sci Eng A 2010;528(1):402–12.
[8] Lian C, Zhuge Y. Optimum mix design of enhanced permeable concrete–An experimental investigation. Constr Build Mater 2010; 24(12):2664–71.
[9] Neithalath N, Sumanasooriya MS, Deo O. Characterizing pore volume, sizes, and connectivity in pervious concretes towards permeability prediction. Mater Charact 2010;61(8):802–13.
[10] Sumanasooriya MS, Deo O, Neithalath N. A particle packing-based material design methodology for pervious concretes. accepted for publication, ACI Mater J; 2011.
[11] Deo O, Neithalath N. Compressive response of pervious concretes proportioned for desired porosities. Constr Build Mater; 2011. <doi:10.1016/j.conbuildmat.2011.04.055>.
[12] Sumanasooriya MS, Deo O, Neithalath N. Computational prediction of elastic properties of enhanced porosity concretes using 3D reconstructed images. In: Proceedings of 9th brittle matrix composites, Warsaw, Poland; October 2009.
[13] Sumanasooriya MS, Bentz DP, Neithalath N. Planar image based reconstruction of pervious concrete pore structure and permeability prediction. ACI Mater J 2010;107(4):413–21.
[14] Neithalath N, Bentz DP, Sumanasooriya MS. Advances in pore structure characterization and performance prediction of pervious concretes. Concr Int 2010;32(5):35–40.
[15] Bentz DP. Virtual pervious concrete: microstructure, percolation, and permeability. ACI Mater J 2008;105(3):297–301.
[16] Neithalath N, Weiss J, Olek J. Characterizing enhanced porosity concrete using electrical impedance to predict acoustic and hydraulic performance. Cem Concr Res 2006;36:2074–85.
[17] Deo O, Sumanasooriya MS, Neithalath N. Proportioning pervious concrete mixtures for desired performance levels. Proceedings of ICI-Asian conference on concrete, IIT Madras, India; December 2010.
[18] Neithalath N. Extracting the performance predictors of enhanced porosity concretes from electrical conductivity spectra. Cem Concr Res 2007;37(5):796–804.
[19] Sumanasooriya MS, Neithalath N. Stereology and morphology based pore structure descriptors of enhanced porosity (pervious) concretes. ACI Mater J 2009;106:429–38.
[20] Low K, Harz D, Neithalath N. Statistical characterization of the pore structure of enhanced porosity concrete. In: Proceedings in CD of the 2008 Concrete Technology Forum, Denver. National Ready Mix Concrete Association; 2008.
[21] ImageJ™ – Image processing and analysis in Java. <http://imagej.nih.gov/ij/download.html>.
[22] Coster M, Chermant J-L. Image analysis and mathematical morphology for civil engineering materials. Cem Concr Res 2001;23:133–51.
[23] Redon C, Chermant L, Chermant JL, Coster M. Automatic image analysis and morphology of fiber reinforced concrete. Cem Concr Compos 1999;21:403–12.
[24] Hu J. Porosity of concrete. Morphological study of model concrete. PhD Thesis. Netherlands, Delft University; 2004.
[25] Garboczi EJ, Bentz DP, Martys NS. Digital images and computer modeling. Experimental methods in the physical sciences. Methods Phys Porous Media 1999;35:1–41.
[26] Berryman JG. Measurement of spatial correlation functions using image processing techniques. J Appl Phys 1985;57:2374–84.
[27] Berryman JG, Blair SC. Use of digital image analysis to estimate fluid permeability of porous materials: application of two-point correlation functions. J Appl Phys 1986;60:1930–8.
[28] Torquato S. Random heterogeneous materials – Microstructure and macroscopic properties. Springer Science and Business Media LLC; 2002.
[29] Berryman JG, Blair SC. Kozeny–Carman relations and image processing methods for estimating Darcy's constant. J Appl Phys 1987;62:2221–8.
[30] Underwood EE. Quantitative stereology. Addison–Wesley Publishing Company; 1968.
[31] Montgomery DC. Design and analysis of experiments. New Jersey: John Wiley & Sons; 2005.
[32] Dias RP, Mota M, Teixeira JA, Yelshin A. Study of ternary glass spherical particle beds: porosity, tortuosity, and permeability. Filtration 2005;5(1):68–75.
[33] Herrick DC, Kennedy WD. Electrical efficiency – a pore geometric theory for interpreting the electrical properties of reservoir rocks. Geophysics 1994;59(6):918–27.
[34] Katz AJ, Thompson AH. Quantitative prediction of permeability in porous rock. Phys Rev B 1986;34(11):8179–81.
[35] Friedman SP, Seaton NA. Critical path analysis of the relationship between permeability and electrical conductivity of three-dimensional pore networks. Water Resour Res 1998;34(7):1703–10.
[36] Plews AG, Atkinson A, McGrane S. Discriminating structural characteristics of starch extrudates through X-ray microtomography using a 3-D watershed algorithm. Int J Food Eng 2009;5(1). doi:10.2202/1556-3758.151.
[37] Le Doussal P. Permeability versus conductivity for porous media with wide distribution of pore sizes. Phys Rev B 1989;39:4816–9.